Published in final edited form as:
J Immunol. 2013 June 15; 190(12): 6468–6477. doi:10.4049/jimmunol.1202583.

Dipeptidyl Peptidase IV Is a Human and Murine Neutrophil Chemorepellent

Sarah E. Herlihy, **Darrell Pilling**, **Anu S. Maharjan**, and **Richard H. Gomer**
Department of Biology, Texas A&M University, College Station, TX 77843

Abstract

In *Dictyostelium discoideum*, AprA is a secreted protein that inhibits proliferation and causes chemorepulsion of *Dictyostelium* cells, yet AprA has little sequence similarity to any human proteins. We found that a predicted structure of AprA has similarity to human dipeptidyl peptidase IV (DPPIV). DPPIV is a serine protease present in extracellular fluids that cleaves peptides with a proline or alanine in the second position. In Insall chambers, DPPIV gradients below, similar to, and above the human serum DPPIV concentration cause movement of human neutrophils away from the higher concentration of DPPIV. A 1% DPPIV concentration difference between the front and back of the cell is sufficient to cause chemorepulsion. Neutrophil speed and viability are unaffected by DPPIV. DPPIV inhibitors block DPPIV-mediated chemorepulsion. In a murine model of acute respiratory distress syndrome, aspirated bleomycin induces a significant increase in the number of neutrophils in the lungs after 3 d. Oropharyngeal aspiration of DPPIV inhibits the bleomycin-induced accumulation of mouse neutrophils. These results indicate that DPPIV functions as a chemorepellent of human and mouse neutrophils, and they suggest new mechanisms to inhibit neutrophil accumulation in acute respiratory distress syndrome.

Chemotaxis is the directed movement of cells due to a gradient of an attractant or repellent. Chemotaxis has been observed in both prokaryotes and eukaryotes (1, 2). In humans, neutrophils show chemotaxis toward bacterial products such as fMLP and toward signals secreted by macrophages and epithelial cells such as IL-8 (3, 4). A large number of chemoattractants have been characterized, whereas relatively few chemorepellents have been identified (5–10).

Dictyostelium cells secrete two proteins, AprA and CfaD, which inhibit *Dictyostelium* cell proliferation (11, 12). Although CfaD has sequence similarity to cathepsin L, AprA shows no significant sequence similarity to eukaryotic proteins (11, 12). We found that AprA also functions as a chemorepellent of *Dictyostelium* cells (13). Wild-type cells in a colony rapidly move away from the dense colony center, whereas AprA knockout cells show no directional movement away from the center of a colony (13, 14). When wild-type cells are placed in a gradient of rAprA, cells show a biased movement away from rAprA (13).

Protein structure prediction can be highly accurate and reveal new functions of a protein (15–20). The protein prediction server I-TASSER uses a multistep process to predict protein structure (15, 17). First, initial models of the structure are generated from the amino acid

Address correspondence and reprint requests to Dr. Richard H. Gomer, Texas A&M University, Department of Biology, Interdisciplinary Life Sciences Building, MS 3474, College Station, TX 77843-3474, rgomer@tamu.edu.

The online version of this article contains supplemental material.

Disclosures: The authors have, through Texas A&M University, applied for a patent on the use of DPPIV as a neutrophil chemorepellent.

sequence (15, 17). The models are then adjusted using Monte Carlo simulations to identify folds with the lowest free energy (15, 17). Finally, spatial constraints and optimal hydrogen bindings are used to adjust the predicted structure (15, 17). The predicted structure can then be used to search for proteins with similar structures (16, 18–20).

Dipeptidyl peptidase IV (DPPIV) is a 110-kDa serine protease that cleaves peptides with a proline or alanine in the second position at the N terminus (21). DPPIV is on the extracellular surface of some lymphocytes and epithelial cells, and a heavily glycosylated soluble form of DPPIV is also found in plasma, serum, cerebrospinal fluid, synovial fluid, semen, and urine (22, 23). DPPIV degrades glucagon-like peptide-1 (24). Drugs that block DPPIV activity also block this degradation and are used to treat type 2 diabetes (24). By activating or deactivating peptide signals, DPPIV affects a large variety of signaling molecules regulating chemotaxis, tissue remodeling, cell adhesion, and other processes (25, 26).

Using the I-TASSER program, we identified structural similarity between *Dictyostelium* AprA and human DPPIV. We show that neutrophils are chemorepulsed by DPPIV, and that this chemorepulsion is dependent on the enzyme activity of DPPIV. In an in vivo model of neutrophil movement, oropharyngeal aspiration of DPPIV reduces neutrophil accumulation in the lungs of bleomycin-treated mice. In this study, we show that DPPIV acts as a chemorepellent of human neutrophils and presents a new potential method to inhibit neutrophil accumulation in tissues.

Materials and Methods

Structure prediction, alignment, and superimposition

The tertiary structure of AprA was predicted using I-TASSER (15–17). The Protein Data Bank file of the predicted AprA structure was input into the Dali server to find similar protein structures and calculate structural similarities (27). The structure of AprA and DPPIV were superimposed using pairwise alignment (http://agknapp.chemie.fu-berlin.de/gplus/) (28, 29).

Neutrophil isolation

Blood was collected from healthy volunteers with specific approval from the Institutional Review Board of Texas A&M University. Written consent was received, and all samples were deidentified before analysis. Neutrophils were isolated from the blood using Lympholyte-poly (Cedarlane Laboratories, Hornby, BC, Canada) following the manufacturer's directions and resuspended in 2% BSA (fraction V, A3059; Sigma-Aldrich) in RPMI 1640 (Lonza).

Neutrophils were further purified using negative selection, as described previously (30). Briefly, neutrophils were depleted of eosinophils, monocytes, and lymphocytes by incubating the cells for 10 min at room temperature with 5 μg/ml anti-human CD244 (BioLegend) and then depleting $CD244^+$ cells with pan Mouse IgG Dynabeads (Invitrogen). Cells were resuspended to a final volume of 1 ml in 2% human albumin-RPMI 1640.

To determine the purity of CD244-depleted neutrophil preparations, cells were resuspended in PBS containing 2% BSA and cell smears were prepared as described previously (31). Cells smears were air dried overnight, fixed in methanol, stained with H&E, and cell morphology was determined by microscopy, as described previously (30).

Human albumin was isolated from human serum (Lonza) using Affi-Gel blue gel beads (Bio-Rad). After washing beads three times with PBS, beads were incubated with serum at

room temperature for 2 h. Beads were collected by centrifugation at 300 × *g* for 2 min and washed with buffer (20 mM Tris, 140 mM NaCl, 2 mM calcium) and the albumin was eluted off overnight with 500 mM NaCl. Albumin was then concentrated and buffer exchanged to Earl's balanced salt solution (Sigma-Aldrich) using a 10-kDa centrifugal filter (Millipore) and stored at 4°C.

Insall chamber assays

Human soluble rDPPIV was purchased from Enzo Life Sciences. To measure the effect of DPPIVon cell displacement, we used Insall chambers, which allows direct visualization of cell movement, as described previously for melanoma cells, *Dictyostelium*, and neutrophils (13, 32, 33). Briefly, 22 × 22-mm glass coverslips were etched with 1 M HCl, rinsed with deionized water, and coated with 20 μg/ml bovine plasma fibronectin (Sigma-Aldrich) for 30 min at 37°C. Coverslips were then washed twice with PBS, and 300 μl neutrophils at 5 × 10^6 cells/ml was allowed to adhere to the coverslip for 15 min at 37°C. We then used an Insall chamber slide, a gift from Robert Insall (32). Two concentric depressions and the separating bridge were filled with 2% BSA-RPMI 1640. The media was removed from the coverslips, which were then placed face down on the chamber. Media was then removed from the outer chamber and was replaced by DPPIV alone, DPPIV inhibitor alone (diprotin A from Enzo Life Sciences or DPPI 1c hydrochloride from Tocris Bioscience), DPPIV plus DPPIV inhibitor (all in 2% BSA-RPMI 1640), or 2% BSA-RPMI 1640. Cells located on the bridge between the square depressions were then filmed as previously described (34), using a ×10 objective for 1 h at 37°C in a humidified 5% CO_2 incubator. Displacement of at least 10 randomly chosen cells per experiment was measured during periods of 10 min. Cell tracking and track analysis was done as previously described (13) with the exception that videos of an hour in length were processed into 10-min segments to yield a TIFF stack of 47 images for analysis (with 13-s intervals between images). Insall chamber assays for pure neutrophils were done with the same procedures except that coverslips were coated with 20 μg/ml human plasma fibronectin (Trevigen) and 2% human albumin-RPMI 1640 was used instead of 2% BSA-RPMI 1640.

For conditioned media assays, neutrophils at 5 × 10^6 cells/ml were incubated with 300 ng/ml DPPIVor an equivalent volume of buffer for 30 min at 37°C in tubes that were precoated with 4% BSA-RPMI 1640. Where indicated, the DPPIV inhibitor DPPI 1c hydrochloride was added to the conditioned medium to a final concentration of 200 nM. Cells were collected by centrifugation at 500 × *g* for 5 min and the supernatant was added to the outside chamber of an Insall chamber. Cells were filmed as described above. Samples of conditioned media were separated on 4–20% PAGE gels (Bio-Rad), transferred to Immobilon-P membranes (Millipore), and membranes were stained with 100 ng/ml anti-human DPPIV Abs (R&D Systems).

Effect of DPPIV peptidase activity on albumin stability

BSA-RPMI 1640 (2%) and 2% human albumin-RPMI 1640 were incubated with 300 ng/ml rDPPIVor an equivalent volume of buffer for 3 h. Samples were taken at 0, 15, 30, 45, 60, and 180 min, mixed with SDS sample buffer, separated on 4–20% PAGE, and then silver stained.

Neutrophil influx in mice

Four-week-old C57BL/6 male mice (The Jackson Laboratory, Bar Harbor, ME) were treated with an oropharyngeal aspiration of 50 μl saline or 3 U/kg bleomycin (Calbiochem) (35). The successful aspiration of bleomycin into the lungs was confirmed by listening for the crackling noise heard after the aspiration. Twenty-four hours following bleomycin aspiration (day 1), mice were treated with an oropharyngeal aspiration of 50 μl 0.9% saline with 0.9

μg rDPPIV (Enzo Life Sciences) or an equal volume of 0.9% saline. Mice were weighed daily and euthanized at day 3 after bleomycin aspiration. Blood was collected by cardiac puncture from the euthanized mice and blood glucose was measured using Accu-Check Active (Roche). The lungs were perfused with 300 μl PBS three times to collect cells by bronchoalveolar lavage (BAL) as described previously (36). The primary BAL cells were collected by centrifugation at 500 × *g* for 10 min. Primary BAL pellets were resuspended in the secondary and tertiary BAL fluid and the combined cells were collected by centrifugation at 500 × *g* for 5 min. The cells were resuspended in 500 μl 4% BSA-PBS and counted with a hemocytometer. Diluted cells (100 μl) were then aliquoted into cytospin funnels and spun onto glass slides (Superfrost Plus white slides; VWR Scientific, West Chester, PA) at 400 rpm for 5 min using a cytospin centrifuge (Shandon, Cheshire, U.K.). These cells were then air-dried and stained with Gill's hematoxylin. More than 200 cells were counted for total cell number, and neutrophils, macrophages, and lymphocytes were identified by morphology. The percentage of neutrophils, macrophages, or lymphocytes was then multiplied by the total number of cells recovered from the BAL to obtain the number of each cell type in the BAL. The mice were used in accordance with guidelines published by the National Institutes of Health, and the protocol was approved by the Texas A&M University Animal Use and Care Committee.

Immunohistochemistry

After BAL, lungs were inflated with prewarmed OCT (VWR Scientific) and then embedded in OCT, frozen on dry ice, and stored at −80°C as described previously (37). Lung tissue sections (5 μm) were prepared and immunohistochemistry was done as described previously (37) except that slides were incubated with 5 μg/ml primary Abs in 4% BSA-PBS for 60 min. Active caspase-3 staining was done overnight at 4°C. The lung sections were stained for Ly6G (BD Biosciences) to detect neutrophils, CD11b (BioLegend) to detect infiltrating macrophages and neutrophils, CD11c (MBL International) to detect lung-resident macrophages and dendritic cells, CD206 (BioLegend) to detect the mannose receptor on macrophages and dendritic cells, and CD107b (Mac3) (BioLegend) to detect alveolar and tissue macrophages and granulocytes, cleaved caspase-3 (Cell Signaling Technologies) to detect activated caspase-3, and isotype-matched mouse or rabbit irrelevant Abs as controls. Slides were then washed three times with PBS for 30 min and incubated with 5 μg/ml biotinylated mouse $F(ab')_2$ anti-rat IgG or 5 μg/ml biotinylated donkey $F(ab')_2$ anti-rabbit IgG in 4% BSA-PBS for 30 min. Slides were then washed three times in PBS for 30 min and incubated with a 1:500 dilution of streptavidin-alkaline phosphatase (Vector Laboratories) in 4% BSA-PBS for 30 min. Staining was developed with a VectorRed alkaline phosphatase kit (Vector Laboratories) for 10 min. Slides were then mounted as described previously (37). Five or ten 450-μm fields of view were counted for Ly6G-stained or active caspase-3–stained positive cells, respectively. Areas containing large blood vessels and bronchioles were excluded from analysis.

Neutrophil survival

Isolated neutrophils were cultured in RPMI 1640 containing 10% (v/v) FBS and 2 mM glutamine in 96-well tissue culture plates at 37°C for 20 h, as described previously (38). Neutrophils were cultured in the presence or absence of 25 ng/ml human IL-8, human TNF-α (both from PeproTech), or 400 ng/ml DPPIV. After 20 h, neutrophils were labeled with annexin V (BioLegend) and propidium iodide (Sigma-Aldrich) according to the manufacturers' instructions to identify early and late stages of cell death. Additionally, cytospin preparations were used to assess for morphological changes associated with apoptosis, as described previously (38–40).

Statistical analysis

Statistics were done using Prism (GraphPad Software, San Diego, CA). One-way ANOVA was used to compare between multiple groups and a Student *t* test was used to compare between two groups.

Results

AprA has structural similarity to the human protein DPPIV

AprA has little sequence similarity to any mammalian protein (11). Using I-TASSER, we generated a predicted structure for AprA (Fig. 1). The Dali server, used to compare protein structures, composes a list of the proteins with the most structural similarity to the query protein. The proteins with the top structural similarities to the predicted structure of AprA were cephalosporin C deacetylase (a β-lactamase from the fungus *Acremonium*), acetyl xylan esterase (from the bacteria *Bacillis pumilus*, which cleaves carboxyl-ester bonds), acylamino acid–releasing enzyme (from the Archaea *Aeropyrum pernix* K1, which cleaves acylated terminal amino acids), and DPPIV (human soluble form, which cleaves terminal amino acids with proline or alanine in the second position). AprA has an 11% structural identity to the entire structure of soluble human DPPIV (Fig. 1, the α/β hydrolase domain of DPPIV is shown). Because DPPIV, similar to AprA, can be found as an extracellular protein, these results suggested that AprA might have functional similarity to DPPIV or vice versa.

Neutrophils show biased movement away from a source of DPPIV

AprA functions as a chemorepellent of *Dictyostelium* cells (13). *Dictyostelium* and neutrophils share many properties of chemotaxis (41, 42). Therefore, we hypothesized that DPPIV may regulate human neutrophil motility owing to its structural similarity to AprA. To examine neutrophil chemotaxis in gradients of DPPIV, we used an Insall chamber. When neutrophil movement was tracked for 10-min periods, there was no bias of movement in the media control (Fig. 2A, Supplemental Fig. 1). A biased movement away from a source of DPPIV was observed (Fig. 2B, Supplemental Fig. 1). Cells were tracked, and the average center of mass observed for the endpoints of cells in each population was determined. The center of mass of cell endpoints showed displacement away from the source of DPPIV (Fig. 2, Supplemental Fig. 1). The concentration of DPPIV in human blood ranges from 400 to 800 ng/ml, or 4.7–9.4 nM (43, 44). Therefore, we tested the ability of DPPIV to affect neutrophil migration above, below, and within this concentration range. Neutrophils showed biased movement away from higher concentrations of rDPPIV in a variety of DPPIV concentration gradients (Table I). An equal concentration of DPPIV in both wells of the chamber resulted in no biased directional movement of neutrophils (Table I). The presence of DPPIV affected directionality, although not in any systematic manner (Table I). Because we used different sets of donors for each gradient concentration, the directionality in the media controls vary somewhat within the different sets of experiments. TNF-α–stimulated neutrophils also migrated away from DPPIV (Table I). For unknown reasons, some of the cells appeared to move toward the higher concentration of DPPIV. In Fig. 2B, two such cells can be seen. The fraction of cells exhibiting this anomalous behavior was not obviously affected by the amount of DPPIV in the gradient (Table I). Collectively, these data indicate that a gradient of DPPIV causes chemorepulsion of neutrophils.

DPPIV gradients affect the probability of directional movement but do not affect cell speed

We also examined the ability of DPPIV to affect cell speed and directional movement using the cell-tracking data. A gradient of DPPIV did not affect cell speed, and speeds were consistent with previous measurements of neutrophil migration (Table II) and were similar

to neutrophil speed observed in gradients on fMLP in an Insall chamber (30.2 ± 3.6 μ/min) (45, 46). P_A and P_T can be defined as the probability that a cell would move away from or toward a source of DPPIV, respectively, in a 13-s interval (13). In gradients of DPPIV, with the exception of a 9.4–23 nM gradient, either P_T was significantly less or P_A was significantly more than the control (Table III). The probability of a cell moving toward or away from DPPIV was similar to the control when equal concentrations were present on either side of the chamber (Table III). DPPIV did not significantly affect P_0, the probability that a cell did not move in a 13-s interval. These results indicate that although a gradient of DPPIV does not significantly affect cell speed, it does affect the movement of a cell toward or away from the source of DPPIV.

Neutrophil chemorepulsion is sensitive to DPPIV enzyme inhibitors

DPPIV enzyme activity has been implicated in the chemotaxis of several types of immune cells through cleavage of human chemokines (25, 47–49). To determine whether DPPIV enzyme activity affects DPPIV-induced neutrophil chemorepulsion, we used two enzyme inhibitors of DPPIV, diprotin A and DPPI 1c hydrochloride (50, 51). The inhibitors alone caused no attraction or repulsion of human neutrophils (Fig. 3). When either of the inhibitors was added with DPPIV, the chemorepulsion of neutrophils away from the source of DPPIV was significantly reduced compared with DPPIV alone (Fig. 3). This suggests that DPPIV inhibitors block the ability of DPPIV to induce neutrophil chemorepulsion.

DPPIV does not appear to cleave albumin

Several possibilities exist to explain why DPPIV enzymatic activity seems to be required for neutrophil chemorepulsion. In addition to DPPIV directly regulating neutrophil chemorepulsion, DPPIV could cleave a component of the media, creating a breakdown component of BSA that acts as a chemorepellent. To determine whether a component of the media was broken down by rDPPIV, BSA-RPMI 1640 or human albumin-RPMI 1640 was incubated with rDPPIV for 3 h. Although BSA is not pure, the human albumin media appear to contain only human albumin and DPPIVas protein components (Fig. 4A, 4B). In both cases, there was no indication of cleavage products accumulating over time or when time points are compared in the presence and absence of rDPPIV (Fig. 4A, 4B).

Purified neutrophils are chemorepulsed by DPPIV

A protein or peptide released by contaminating cells into the media and then cleaved by DPPIV could also act as the chemorepellent. Neutrophils were further purified after isolation, resuspended in pure human albumin, and assayed for chemorepulsion from DPPIV. Both the number of contaminating eosinophils and monocytes in the neutrophil preparation decreased significantly following depletion (Fig. 4C). Neutrophils were 97% pure following CD244 depletion, making a gradient of attractant or repellent from remaining contaminating cells unlikely (Fig. 4C). Pure neutrophils showed a biased movement away from rDPPIV (Fig. 4D). These data suggest that it is unlikely that DPPIV cleaves a component of the media or from contaminating cells to induce chemorepulsion.

Conditioned medium from neutrophils does not affect chemorepulsion

Proteases on the neutrophil surface could create a neutrophil chemorepellent or cleave a breakdown component of the media that acts as a chemorepellent. Additionally, neutrophils could be releasing a chemorepellent or chemoattractant that is then affected by DPPIV. To determine whether neutrophil proteins are responsible for the chemorepulsion effect, neutrophils were incubated with DPPIV or an equivalent volume of buffer for 30 min at 37°C. Neutrophils were then collected by centrifugation, the conditioned media were recovered, and media from the outer chamber of the Insall chamber were replaced with these

conditioned media. Half of the conditioned medium from cells preincubated with DPPIV was mixed with the DPPIV inhibitor DPPI 1c hydrochloride immediately before addition to the Insall chamber. Conditioned media from buffer-treated cells or conditioned media from DPPIV-treated cells that were mixed with the inhibitor failed to promote chemorepulsion of neutrophils (Fig. 5A). Conditioned media from DPPIV-treated cells did promote chemorepulsion of neutrophils (Fig. 5A). As determined by Western blots stained with anti-DPPIV Abs, there was no detectable DPPIV present in conditioned media from buffer-treated cells, whereas there was DPPIV present in the conditioned media from DPPIV-treated cells (Fig. 5B). Taken together, these data suggest that DPPIV promotes neutrophil chemorepulsion, rather than cleaving a component of the media or a substrate secreted from cells.

DPPIV reduces the number of neutrophils in lungs of mice treated with bleomycin

Oropharyngeal aspiration of bleomycin in mice causes neutrophils to accumulate in the lungs within 24 h of bleomycin administration (52). If DPPIV functions as a neutrophil chemorepellent, then administering DPPIV to a tissue could drive neutrophils out of the tissue or prevent their entry. We examined the ability of DPPIV to affect neutrophil accumulation in the lungs of bleomycin-treated mice. Assuming the volume of liquid in the airways of mouse lungs is not >0.1 ml, administering 0.9 μg DPPIV creates a DPPIV concentration considerably greater than the DPPIV serum concentration of 0.4 μg/ml (53). Mice were treated with bleomycin on day 0 and were treated with aspirated rDPPIV or an equivalent volume of saline on day 1. Bleomycin is metabolized and excreted within 24 h, so the DPPIV treatment at 24 h does not block the effect of bleomycin (54, 55). Three days after bleomycin treatment, mice were euthanized and weakly adhered cells from the airways were collected by BAL. Although the BAL from DPPIV-treated mice appeared to have fewer total number of cells than did that from mice given bleomycin alone, this difference was not significant (Fig. 6A). BALs from mice given rDPPIV following saline had significantly fewer cells than mice given saline or bleomycin alone (Fig. 6A). Cell morphology was used to determine the total number of neutrophils, macrophages, and lymphocytes in the BAL. Significantly fewer neutrophils were present in the BALs from bleomycin plus rDPPIV– and saline plus rDPPIV–treated mice compared with mice treated with bleomycin alone (Fig. 6B). There was no difference in total macrophage or lymphocyte numbers in the BAL between DPPIV-treated mice and their untreated counterparts (Fig. 6B). Following BAL, lungs were sectioned and stained with anti-mouse Ly6G to detect neutrophils. There were significantly fewer $Ly6G^+$ cells in the post-BAL lungs of mice treated with bleomycin and then treated with DPPIV on day 1 than the post-BAL lungs of mice treated with bleomycin alone (Fig. 6C, 6D). There was no difference in the numbers of CD11b, CD11c, CD206, or CD107b (Mac3)-positive cells in the lungs of mice treated with bleomycin compared with those treated with bleomycin and then treated with DPPIV (Fig. 6E), suggesting that the effect of DPPIV is specific to neutrophils.

DPPIV regulates glucagon-like peptide-1, which regulates glucose levels in the blood (56). Inhibiting DPPIV affects glucose levels in mice (57). To determine whether oropharyngeal aspiration of DPPIV at day 1 affected weight gain or serum glucose levels, we measured weight change for 3 d and measured glucose levels in the blood of mice euthanized on day 3. Although not statistically significant, DPPIV administration appeared to rescue the weight loss caused by bleomycin and had no significant impact on weight gain when administered on day 1 to mice given saline on day 0 (Supplemental Fig. 2A). Additionally, DPPIV administration had no significant effect on serum glucose levels at day 3 (Supplemental Fig. 2B). Taken together, our results indicate that DPPIV reduces the accumulation of neutrophils in the lungs of mice but does not cause significant changes in weight or serum glucose levels 2 d after administration.

DPPIV does not promote or inhibit neutrophil survival

The number of cells in any tissue is dependent on four factors: proliferation, death, recruitment, and emigration (58). Because neutrophils are terminally differentiated cells, proliferation is not likely to regulate neutrophil numbers in an inflammatory environment. To determine whether the reduction in the number of neutrophils in DPPIV-treated lungs was due to altered cell survival, we cultured human neutrophils in the presence or absence of DPPIV for 20 h. In the absence of exogenous proteins, most neutrophils were apoptotic, as determined by annexin V staining and morphological changes (Fig. 7A, 7B). The addition of DPPIV had no significant effect on neutrophil survival (Fig. 7A–C). To determine whether DPPIV was regulating neutrophil survival in vivo, we stained lung sections with Abs against active caspase-3. Similar to previous observations in the presence or absence of bleomycin, there was no difference in the number of cells labeled with active caspase-3 Abs with the addition of DPPIV (Fig. 7D) (59). These data indicate that the reduction in the number of neutrophils in the lungs of mice following DPPIV administration is unlikely to be due to increased neutrophil cell death.

Discussion

We previously characterized AprA as an endogenous chemorepellent of *Dictyostelium* cells (13). In this study, we identified structural similarities between AprA and human DPPIV and found that DPPIV appears to act as a neutrophil chemorepellent at physiological concentrations.

In the Insall chambers, we observed a strong DPPIV chemorepellent effect using a 0–100 ng/ml (0–1.2 nM) gradient. The gradient in the Insall chamber forms over a 970-μm gap. Making the first-order assumption that the gradient is linear, DPPIV is effective at 0.10 ng/ml/μm, or 0.0012 nM/μm. With an observed average neutrophil length of 10.5 μm (consistent with previous observations) (60), a cell in the middle of the gradient would correspond to a difference of 1.1 ng over the length of the cell at a place where the average DPPIV concentration is 50 ng/ml. This would then represent a 2.2% difference in the DPPIV concentration between the front and the back of the cell. For the 4.7– 11.7 nM and the 9.4–23 nM gradients, the difference is 0.9%. This is similar to the 1.25% concentration difference of cAMP that induces chemotaxis for aggregating *Dictyostelium* cells (45), or the 1% fMLP concentration gradient that induces neutrophil chemotaxis (61).

For unknown reasons, we observed that for all of the DPPIV gradients in the Insall chambers, ~17% of the neutrophils showed movement toward the source of DPPIV during 10 min. There was no obvious difference in the percentage of cells moving toward DPPIV as a function of the DPPIV concentration gradient. This effect is strikingly similar to the observation that 17% of *Dictyostelium* cells also move toward a source of AprA in the Insall chambers (13). At the lowest gradient concentration used, the DPPIV concentration at the middle of the gradient was 0.6 nM, or ~110 DPPIV molecules per cell volume in the extracellular environment. By Poisson statistics, there could be momentary conditions where the cell does not detect the gradient or detects an “opposite” gradient. However, during 10 min all cells should detect the gradient. As the percentage of non-neutrophils in both isolated and purified neutrophils is <17% of the total population, some portion of the backward-moving cells must be neutrophils. The existence of cells moving backward thus indicates an unknown heterogeneity in both *Dictyostelium* cells and human neutrophils.

Inhibitors that block the active site of DPPIV also blocked the ability of DPPIV to act as a chemorepellent. It is possible that the inhibitors disrupt the DPPIV structure and therefore disturb its ability to act as a ligand for a chemorepellent receptor. However, the crystal structure of human DPPIVin a complex with diprotin A shows no significant structural

difference compared with DPPIV alone (62). This suggests that the inhibitors block chemorepulsion in some other manner, such as blocking the ability to cleave something in the assay medium. In the Insall chamber assays, neutrophils were in RPMI 1640 containing BSA or human albumin on a fibronectin surface. The only known enzymatic activity of DPPIV is cleavage of two amino acids from the N terminus of a protein if the second amino acid is a proline or alanine (26). RPMI 1640 does not contain proteins, and BSA and human albumin do not have a proline or an alanine as the second amino acid. Additionally, no cleavage products of BSA or human albumin were seen following incubation with rDPPIV for 3 h. DPPIV does not cleave fibronectin (63). Following CD244 depletion, neutrophils were 97% pure and rDPPIV was still able to cause repulsion, indicating that a factor secreted by cells contaminating the neutrophil preparation is not likely responsible for the effect. There are no known neutrophil-secreted neutrophil chemoattractants that are, or could be, affected by DPPIV (25, 64–68). Conditioned media from neutrophils incubated with buffer alone did not cause attraction or repulsion of neutrophils, supporting this idea. Conditioned media from neutrophils incubated with DPPIV caused chemorepulsion of neutrophils. The chemorepulsive activity of the conditioned media was lost with the addition of a DPPIV inhibitor, suggesting that the chemorepulsive activity in the conditioned media is due specifically to the presence of DPPIV activity. Although DPPIV-induced neutrophil chemorepulsion appears to require the DPPIV active site, the chemorepulsion does not appear to be caused by DPPIV's enzymatic activity on material in the medium, on chemoattractants or repellents, or by components from cells.

DPPIV knockout mice have been generated (53) and rat strains lacking DPPIV have been identified (69, 70). DPPIV-deficient animals have normal blood levels of most leukocytes, including neutrophils (71–73). Arthritic joints in mammals contain abnormally high numbers of neutrophils (74). DPPIV knockout mice have increased severity of experimentally induced arthritis, with a 2.4-fold increase in the number of cells in the joint (75). A 2-fold increase in neutrophils occurs in OVA-induced lung inflammation in DPPIV-deficient rats compared with normal rats (76). Reduced levels of DPPIV correlate with increased inflammation in the joints of rheumatoid arthritis patients (77). The increased inflammation observed in DPPIV-deficient situations has been assumed to be due to a persistent chemokine presence, as DPPIV was not present to cleave those chemokines that have an alanine or proline as the second amino acid (78).

We found that oropharyngeal aspiration of DPPIV caused a reduction in the accumulation of neutrophils, but not other immune cells, in the lungs of mice treated with bleomycin, suggesting that the chemorepulsive effect of DPPIV is specific to neutrophils. Additionally, the reduction in neutrophils was not due to increased neutrophil death. Our data suggests an alternative hypothesis to the persistence of chemokines in a tissue. We hypothesize that DPPIV acts directly as a neutrophil chemorepellent. Following neutrophil influx, activated T cells enter a site of inflammation (79). Activated T cells highly express membrane DPPIV, and extracellular DPPIV is thought to be cleaved from the membrane of T cells (22). An increase in extracellular DPPIV could promote neutrophil egress from the inflammatory site. In the resolution of zebrafish wounds, neutrophils are able to move out of the tissue and back into the vasculature (80). An intriguing possibility is that T cell–released DPPIV may help cause the egress of neutrophils out of the lung tissue to resolve lung inflammation. Some lung diseases such as acute respiratory distress syndrome involve an excess number of neutrophils in the lungs (81). The ability of DPPIV to induce neutrophil chemorepulsion suggests the existence of new mechanisms that may be used to treat these diseases.

Supplementary Material

Refer to Web version on PubMed Central for supplementary material.

Acknowledgments

We thank Robert Insall for the gift of the Insall chamber, and the staff at Beutel Student Health Services for the phlebotomy work. We also thank Jonathan Phillips and Dr. Criscitiello for their comments on the manuscript.

References

1. Baker MD, Wolanin PM, Stock JB. Signal transduction in bacterial chemotaxis. Bioessays. 2006; 28:9–22. [PubMed: 16369945]
2. Swaney KF, Huang CH, Devreotes PN. Eukaryotic chemotaxis: a network of signaling pathways controls motility, directional sensing, and polarity. Annu Rev Biophys. 2010; 39:265–289. [PubMed: 20192768]
3. Leonard EJ, Yoshimura T. Neutrophil attractant/activation protein-1 (NAP-1 [interleukin-8]). Am J Respir Cell Mol Biol. 1990; 2:479–486. [PubMed: 2189453]
4. Crossley LJ. Neutrophil activation by fMLP regulates FOXO (forkhead) transcription factors by multiple pathways, one of which includes the binding of FOXO to the survival factor Mcl-1. J Leukoc Biol. 2003; 74:583–592. [PubMed: 12960271]
5. Colamarino SA, Tessier-Lavigne M. The axonal chemoattractant netrin-1 is also a chemorepellent for trochlear motor axons. Cell. 1995; 81:621–629. [PubMed: 7758116]
6. Masuda T, Watanabe K, Sakuma C, Ikenaka K, Ono K, Yaginuma H. Netrin-1 acts as a repulsive guidance cue for sensory axonal projections toward the spinal cord. J Neurosci. 2008; 28:10380–10385. [PubMed: 18842897]
7. Zaki M, Andrew N, Insall RH. *Entamoeba histolytica* cell movement: a central role for self-generated chemokines and chemorepellents. Proc Natl Acad Sci USA. 2006; 103:18751–18756. [PubMed: 17132728]
8. Messersmith EK, Leonardo ED, Shatz CJ, Tessier-Lavigne M, Goodman CS, Kolodkin AL. Semaphorin III can function as a selective chemorepellent to pattern sensory projections in the spinal cord. Neuron. 1995; 14:949–959. [PubMed: 7748562]
9. Vianello F, Olszak IT, Poznansky MC. Fugetaxis: active movement of leukocytes away from a chemokinetic agent. J Mol Med (Berl). 2005; 83:752–763. [PubMed: 16142473]
10. Tharp WG, Yadav R, Irimia D, Upadhyaya A, Samadani A, Hurtado O, Liu SY, Munisamy S, Brainard DM, Mahon MJ, et al. Neutrophil chemorepulsion in defined interleukin-8 gradients in vitro and in vivo. J Leukoc Biol. 2006; 79:539–554. [PubMed: 16365152]
11. Brock DA, Gomer RH. A secreted factor represses cell proliferation in *Dictyostelium*. Development. 2005; 132:4553–4562. [PubMed: 16176950]
12. Bakthavatsalam D, Brock DA, Nikravan NN, Houston KD, Hatton RD, Gomer RH. The secreted *Dictyostelium* protein CfaD is a chalone. J Cell Sci. 2008; 121:2473–2480. [PubMed: 18611962]
13. Phillips JE, Gomer RH. A secreted protein is an endogenous chemorepellant in *Dictyostelium discoideum*. Proc Natl Acad Sci USA. 2012; 109:10990–10995. [PubMed: 22711818]
14. Phillips JE, Gomer RH. The ROCO kinase QkgA is necessary for proliferation inhibition by autocrine signals in*Dictyostelium discoideum*. Eukaryot Cell. 2010; 9:1557–1565. [PubMed: 20709790]
15. Roy A, Kucukural A, Zhang Y. I-TASSER: a unified platform for automated protein structure and function prediction. Nat Protoc. 2010; 5:725–738. [PubMed: 20360767]
16. Roy A, Yang J, Zhang Y. COFACTOR: an accurate comparative algorithm for structure-based protein function annotation. Nucleic Acids Res. 2012; 40(Web Server issue):W471–W477. 10.1093/nar/gks372. [PubMed: 22570420]
17. Zhang Y. I-TASSER server for protein 3D structure prediction. BMC Bioinformatics. 2008; 9:40. [PubMed: 18215316]
18. Whisstock JC, Lesk AM. Prediction of protein function from protein sequence and structure. Q Rev Biophys. 2003; 36:307–340. [PubMed: 15029827]
19. Lee D, Redfern O, Orengo C. Predicting protein function from sequence and structure. Nat Rev Mol Cell Biol. 2007; 8:995–1005. [PubMed: 18037900]

20. Kim SH, Shin DH, Choi IG, Schulze-Gahmen U, Chen S, Kim R. Structure-based functional inference in structural genomics. J Struct Funct Genomics. 2003; 4:129–135. [PubMed: 14649297]
21. Walborg EF Jr, Tsuchida S, Weeden DS, Thomas MW, Barrick A, McEntire KD, Allison JP, Hixson DC. Identification of dipeptidyl peptidase IV as a protein shared by the plasma membrane of hepatocytes and liver biomatrix. Exp Cell Res. 1985; 158:509–518. [PubMed: 3891389]
22. Cordero OJ, Salgado FJ, Nogueira M. On the origin of serum CD26 and its altered concentration in cancer patients. Cancer Immunol Immunother. 2009; 58:1723–1747. [PubMed: 19557413]
23. Kotacková L, Baláziová E, Sedo A. Expression pattern of dipeptidyl peptidase IV activity and/or structure homologues in cancer. Folia Biol (Praha). 2009; 55:77–84. [PubMed: 19545486]
24. Nauck MA, Vardarli I, Deacon CF, Holst JJ, Meier JJ. Secretion of glucagon-like peptide-1 (GLP-1) in type 2 diabetes: what is up, what is down? Diabetologia. 2011; 54:10–18. [PubMed: 20871975]
25. Struyf S, Proost P, Van Damme J. Regulation of the immune response by the interaction of chemokines and proteases. Adv Immunol. 2003; 81:1–44. [PubMed: 14711052]
26. Chen WT, Kelly T, Ghersi G. DPPIV, seprase, and related serine peptidases in multiple cellular functions. Curr Top Dev Biol. 2003; 54:207–232. [PubMed: 12696751]
27. Holm L, RosenstrÖm P. Dali server: conservation mapping in 3D. Nucleic Acids Res. 2010; 38(Web Server issue):W545–W549. [PubMed: 20457744]
28. Kolbeck B, May P, Schmidt-Goenner T, Steinke T, Knapp EW. Connectivity independent protein-structure alignment: a hierarchical approach. BMC Bioinformatics. 2006; 7:510. [PubMed: 17118190]
29. Guerler A, Knapp EW. Novel protein folds and their nonsequential structural analogs. Protein Sci. 2008; 17:1374–1382. [PubMed: 18583523]
30. Hansel TT, Pound JD, Pilling D, Kitas GD, Salmon M, Gentle TA, Lee SS, Thompson RA. Purification of human blood eosinophils by negative selection using immunomagnetic beads. J Immunol Methods. 1989; 122:97–103. [PubMed: 2547875]
31. Pilling D, Kitas GD, Salmon M, Bacon PA. The kinetics of interaction between lymphocytes and magnetic polymer particles. J Immunol Methods. 1989; 122:235–241. [PubMed: 2794518]
32. Muinonen-Martin AJ, Veltman DM, Kalna G, Insall RH. An improved chamber for direct visualisation of chemotaxis. PLoS ONE. 2010; 5:e15309. [PubMed: 21179457]
33. Itakura A, Verbout NG, Phillips KG, Insall RH, Gailani D, Tucker EI, Gruber A, McCarty OJ. Activated factor XI inhibits chemotaxis of polymorphonuclear leukocytes. J Leukoc Biol. 2011; 90:923–927. [PubMed: 21807745]
34. Ochsner SA, Day AJ, Rugg MS, Breyer RM, Gomer RH, Richards JS. Disrupted function of tumor necrosis factor-α-stimulated gene 6 blocks cumulus cell-oocyte complex expansion. Endocrinology. 2003; 144:4376–4384. [PubMed: 12959984]
35. Lakatos HF, Burgess HA, Thatcher TH, Redonnet MR, Hernady E, Williams JP, Sime PJ. Oropharyngeal aspiration of a silica suspension produces a superior model of silicosis in the mouse when compared to intratracheal instillation. Exp Lung Res. 2006; 32:181–199. [PubMed: 16908446]
36. Corteling R, Wyss D, Trifilieff A. In vivo models of lung neutrophil activation. Comparison of mice and hamsters. BMC Pharmacol. 2002; 2:1. [PubMed: 11806755]
37. Pilling D, Roife D, Wang M, Ronkainen SD, Crawford JR, Travis EL, Gomer RH. Reduction of bleomycin-induced pulmonary fibrosis by serum amyloid P. J Immunol. 2007; 179:4035–4044. [PubMed: 17785842]
38. Scheel-Toellner D, Wang K, Henriquez NV, Webb PR, Craddock R, Pilling D, Akbar AN, Salmon M, Lord JM. Cytokine-mediated inhibition of apoptosis in non-transformed T cells and neutrophils can be dissociated from protein kinase B activation. Eur J Immunol. 2002; 32:486–493. [PubMed: 11828365]
39. Pilling D, Akbar AN, Girdlestone J, Orteu CH, Borthwick NJ, Amft N, Scheel-Toellner D, Buckley CD, Salmon M. Interferon-β mediates stromal cell rescue of T cells from apoptosis. Eur J Immunol. 1999; 29:1041–1050. [PubMed: 10092109]

40. Buckley CD, Pilling D, Henriquez NV, Parsonage G, Threlfall K, Scheel-Toellner D, Simmons DL, Akbar AN, Lord JM, Salmon M. RGD peptides induce apoptosis by direct caspase-3 activation. Nature. 1999; 397:534–539. [PubMed: 10028971]
41. Wang Y, Chen CL, Iijima M. Signaling mechanisms for chemotaxis. Dev Growth Differ. 2011; 53:495–502. [PubMed: 21585354]
42. Wang F. The signaling mechanisms underlying cell polarity and chemotaxis. Cold Spring Harb Perspect Biol. 2009; 1:a002980. [PubMed: 20066099]
43. Aso Y, Ozeki N, Terasawa T, Naruse R, Hara K, Suetsugu M, Takebayashi K, Shibazaki M, Haruki K, Morita K, Inukai T. Serum level of soluble CD26/dipeptidyl peptidase-4 (DPP-4) predicts the response to sitagliptin, a DPP-4 inhibitor, in patients with type 2 diabetes controlled inadequately by metformin and/or sulfonylurea. Transl Res. 2012; 159:25–31. [PubMed: 22153807]
44. Cordero OJ, Ayude D, Nogueira M, Rodriguez-Berrocal FJ, de la Cadena MP. Preoperative serum CD26 levels: diagnostic efficiency and predictive value for colorectal cancer. Br J Cancer. 2000; 83:1139–1146. [PubMed: 11027426]
45. Zigmond SH. Ability of polymorphonuclear leukocytes to orient in gradients of chemotactic factors. J Cell Biol. 1977; 75:606–616. [PubMed: 264125]
46. Liu X, Ma B, Malik AB, Tang H, Yang T, Sun B, Wang G, Minshall RD, Li Y, Zhao Y, et al. Bidirectional regulation of neutrophil migration by mitogen-activated protein kinases. Nat Immunol. 2012; 13:457–464. [PubMed: 22447027]
47. Christopherson KW II, Hangoc G, Broxmeyer HE. Cell surface peptidase CD26/dipeptidylpeptidase IV regulates CXCL12/stromal cell-derived factor-1 α-mediated chemotaxis of human cord blood $CD34^+$ progenitor cells. J Immunol. 2002; 169:7000–7008. [PubMed: 12471135]
48. Lambeir AM, Proost P, Durinx C, Bal G, Senten K, Augustyns K, Scharpé S, Van Damme J, De Meester I. Kinetic investigation of chemokine truncation by CD26/dipeptidyl peptidase IV reveals a striking selectivity within the chemokine family. J Biol Chem. 2001; 276:29839–29845. [PubMed: 11390394]
49. Proost P, Menten P, Struyf S, Schutyser E, De Meester I, Van Damme J. Cleavage by CD26/dipeptidyl peptidase IV converts the chemokine LD78β into a most efficient monocyte attractant and CCR1 agonist. Blood. 2000; 96:1674–1680. [PubMed: 10961862]
50. Wright SW, Ammirati MJ, Andrews KM, Brodeur AM, Danley DE, Doran SD, Lillquist JS, McClure LD, McPherson RK, Orena SJ, et al. *cis*-2,5-dicyanopyrrolidine inhibitors of dipeptidyl peptidase IV: synthesis and in vitro, in vivo, and X-ray crystallographic characterization. J Med Chem. 2006; 49:3068–3076. [PubMed: 16722626]
51. Rahfeld J, Schierhorn M, Hartrodt B, Neubert K, Heins J. Are diprotin A (Ile-Pro-Ile) and diprotin B (Val-Pro-Leu) inhibitors or substrates of dipeptidyl peptidase IV? Biochim Biophys Acta. 1991; 1076:314–316. [PubMed: 1671823]
52. Moore BB, Hogaboam CM. Murine models of pulmonary fibrosis. Am J Physiol Lung Cell Mol Physiol. 2008; 294:L152–L160. [PubMed: 17993587]
53. Marguet D, Baggio L, Kobayashi T, Bernard AM, Pierres M, Nielsen PF, Ribel U, Watanabe T, Drucker DJ, Wagtmann N. Enhanced insulin secretion and improved glucose tolerance in mice lacking CD26. Proc Natl Acad Sci USA. 2000; 97:6874–6879. [PubMed: 10823914]
54. Lazo JS, Pham ET. Pulmonary fate of [3H]bleomycin A2 in mice. J Pharmacol Exp Ther. 1984; 228:13–18. [PubMed: 6198509]
55. Giri SN. Pharmacokinetics, subcellular distribution, and covalent binding of [3H]bleomycin in hamsters after intratracheal administration. Exp Mol Pathol. 1986; 45:207–220. [PubMed: 2429861]
56. Kieffer TJ, McIntosh CH, Pederson RA. Degradation of glucose-dependent insulinotropic polypeptide and truncated glucagon-like peptide 1 in vitro and in vivo by dipeptidyl peptidase IV. Endocrinology. 1995; 136:3585–3596. [PubMed: 7628397]
57. Reimer MK, Holst JJ, Ahrén B. Long-term inhibition of dipeptidyl peptidase IV improves glucose tolerance and preserves islet function in mice. Eur J Endocrinol. 2002; 146:717–727. [PubMed: 11980629]

58. Buckley CD, Pilling D, Lord JM, Akbar AN, Scheel-Toellner D, Salmon M. Fibroblasts regulate the switch from acute resolving to chronic persistent inflammation. Trends Immunol. 2001; 22:199–204. [PubMed: 11274925]
59. Goto H, Ledford JG, Mukherjee S, Noble PW, Williams KL, Wright JR. The role of surfactant protein A in bleomycin-induced acute lung injury. Am J Respir Crit Care Med. 2010; 181:1336–1344. [PubMed: 20167853]
60. Li Z, Dong X, Wang Z, Liu W, Deng N, Ding Y, Tang L, Hla T, Zeng R, Li L, Wu D. Regulation of PTEN by Rho small GTPases. Nat Cell Biol. 2005; 7:399–404. [PubMed: 15793569]
61. Skoge M, Adler M, Groisman A, Levine H, Loomis WF, Rappel WJ. Gradient sensing in defined chemotactic fields. Integr Biol (Camb). 2010; 2:659–668. [PubMed: 20882228]
62. Hiramatsu H, Yamamoto A, Kyono K, Higashiyama Y, Fukushima C, Shima H, Sugiyama S, Inaka K, Shimizu R. The crystal structure of human dipeptidyl peptidase IV (DPPIV) complex with diprotin. A Biol Chem. 2004; 385:561–564.
63. Bermpohl F, LÖster K, Reutter W, Baum O. Rat dipeptidyl peptidase IV (DPP IV) exhibits endopeptidase activity with specificity for denatured fibrillar collagens. FEBS Lett. 1998; 428:152–156. [PubMed: 9654125]
64. Tomazella GG, da Silva I, Laure HJ, Rosa JC, Chammas R, Wiker HG, de Souza GA, Greene LJ. Proteomic analysis of total cellular proteins of human neutrophils. Proteome Sci. 2009; 7:32. [PubMed: 19719850]
65. Lominadze G, Powell DW, Luerman GC, Link AJ, Ward RA, McLeish KR. Proteomic analysis of human neutrophil granules. Mol Cell Proteomics. 2005; 4:1503–1521. [PubMed: 15985654]
66. de Souza Castro M, de Sá NM, Gadelha RP, de Sousa MV, Ricart CA, Fontes B, Fontes W. Proteome analysis of resting human neutrophils. Protein Pept Lett. 2006; 13:481–487. [PubMed: 16800802]
67. Jethwaney D, Islam MR, Leidal KG, de Bernabe DB, Campbell KP, Nauseef WM, Gibson BW. Proteomic analysis of plasma membrane and secretory vesicles from human neutrophils. Proteome Sci. 2007; 5:12. [PubMed: 17692124]
68. Uriarte SM, Powell DW, Luerman GC, Merchant ML, Cummins TD, Jog NR, Ward RA, McLeish KR. Comparison of proteins expressed on secretory vesicle membranes and plasma membranes of human neutrophils. J Immunol. 2008; 180:5575–5581. [PubMed: 18390742]
69. Karl T, Chwalisz WT, Wedekind D, Hedrich HJ, Hoffmann T, Jacobs R, Pabst R, von HÖrsten S. Localization, transmission, spontaneous mutations, and variation of function of the Dpp4 (dipeptidyl-peptidase IV; CD26) gene in rats. Regul Pept. 2003; 115:81–90. [PubMed: 12972323]
70. Shibayama K, Nakamura T, Kinoshita I, Ueki Y, Nakao H, Eguchi K, Tsujihata M, Nagataki S. Remarkable increase in CD26-positive T cells in patients with human T lymphotropic virus type I (HTLV-I) associated myelopathy. Intern Med. 1992; 31:1081–1083. [PubMed: 1358283]
71. Christopherson KW, Cooper S, Hangoc G, Broxmeyer HE. CD26 is essential for normal G-CSF-induced progenitor cell mobilization as determined by $CD26^{-/-}$ mice. Exp Hematol. 2003; 31:1126–1134. [PubMed: 14585379]
72. Kidd S, Bueso-Ramos C, Jagan S, Paganessi LA, Boggio LN, Fung HC, Gregory SA, Christopherson KW 2nd. In vivo expansion of the megakaryocyte progenitor cell population in adult CD26-deficient mice. Exp Hematol. 2011; 39:580–590.e1. [PubMed: 21291952]
73. Frerker N, Raber K, Bode F, Skripuletz T, Nave H, Klemann C, Pabst R, Stephan M, Schade J, Brabant G, et al. Phenotyping of congenic dipeptidyl peptidase 4 (DP4) deficient Dark Agouti (DA) rats suggests involvement of DP4 in neuro-, endocrine, and immune functions. Clin Chem Lab Med. 2009; 47:275–287. [PubMed: 19327106]
74. Wright HL, Moots RJ, Bucknall RC, Edwards SW. Neutrophil function in inflammation and inflammatory diseases. Rheumatology (Oxford). 2010; 49:1618–1631. [PubMed: 20338884]
75. Busso N, Wagtmann N, Herling C, Chobaz-Péclat V, Bischof-Delaloye A, So A, Grouzmann E. Circulating CD26 is negatively associated with inflammation in human and experimental arthritis. Am J Pathol. 2005; 166:433–442. [PubMed: 15681827]
76. Schmiedl A, Krainski J, SchwichtenhÖvel F, Schade J, Klemann C, Raber KA, Zscheppang K, Beekmann T, Acevedo C, Glaab T, et al. Reduced airway inflammation in CD26/DPP4-deficient

F344 rats is associated with altered recruitment patterns of regulatory T cells and expression of pulmonary surfactant proteins. Clin Exp Allergy. 2010; 40:1794–1808. [PubMed: 20560982]

77. Kamori M, Hagihara M, Nagatsu T, Iwata H, Miura T. Activities of dipeptidyl peptidase II, dipeptidyl peptidase IV, prolyl endopeptidase, and collagenase-like peptidase in synovial membrane from patients with rheumatoid arthritis and osteoarthritis. Biochem Med Metab Biol. 1991; 45:154–160. [PubMed: 1679339]
78. Yazbeck R, Howarth GS, Abbott CA. Dipeptidyl peptidase inhibitors, an emerging drug class for inflammatory disease? Trends Pharmacol Sci. 2009; 30:600–607. [PubMed: 19837468]
79. Barbul A, Breslin RJ, Woodyard JP, Wasserkrug HL, Efron G. The effect of in vivo T helper and T suppressor lymphocyte depletion on wound healing. Ann Surg. 1989; 209:479–483. [PubMed: 2522759]
80. Mathias JR, Perrin BJ, Liu TX, Kanki J, Look AT, Huttenlocher A. Resolution of inflammation by retrograde chemotaxis of neutrophils in transgenic zebrafish. J Leukoc Biol. 2006; 80:1281–1288. [PubMed: 16963624]
81. Matthay MA, Zemans RL. The acute respiratory distress syndrome: pathogenesis and treatment. Annu Rev Pathol. 2011; 6:147–163. [PubMed: 20936936]

Abbreviations used in this article

BAL	bronchoalveolar lavage
DPPIV	dipeptidyl peptidase IV

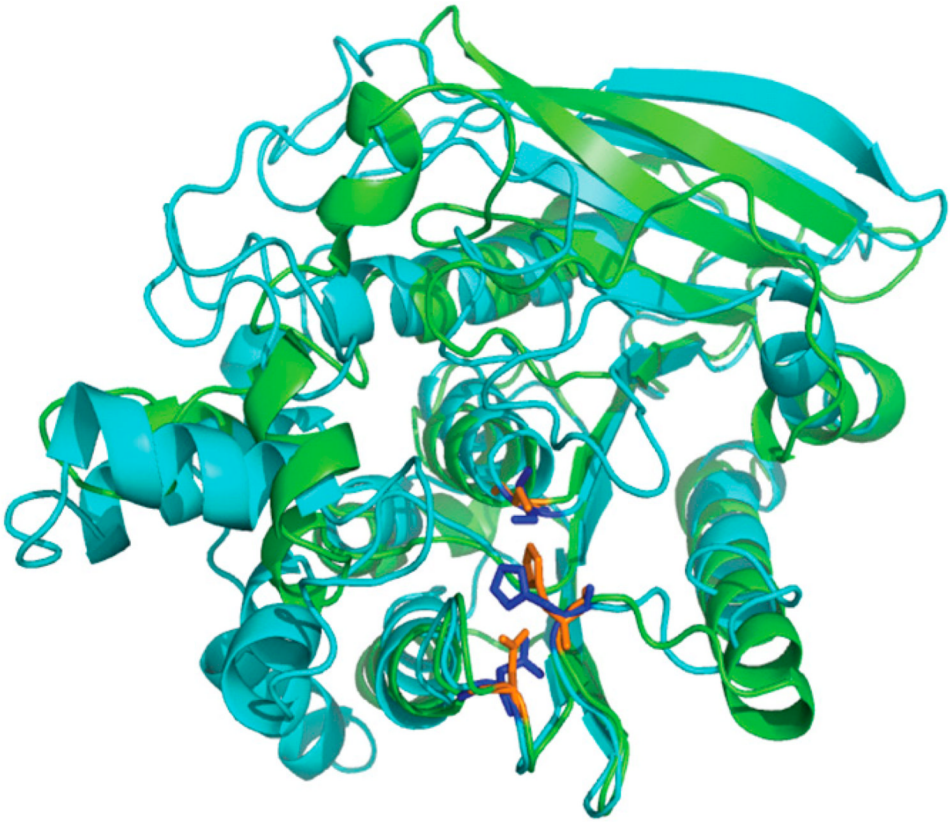

Figure 1.

Superimposition of the predicted structure of AprA with the structure of the α/β hydrolase domain of human DPPIV. The catalytic domains of DPPIV (the α/β hydrolase domain of Protein Data Bank ID 1J2E) and AprA (predicted structure) were superimposed and the catalytic triads highlighted. The α/β hydrolase domain of DPPIV is shown in green and its catalytic triad (Asp^{708}, His^{740}, and Ser^{630}) is orange. The predicted structure of AprA is shown in cyan and its potential catalytic triad (Asp^{288}, His^{319}, and Ser^{195}) is blue. The β-propeller domain of DPPIV was removed for simplicity because the predicted structure of AprA had no overlap with this domain.

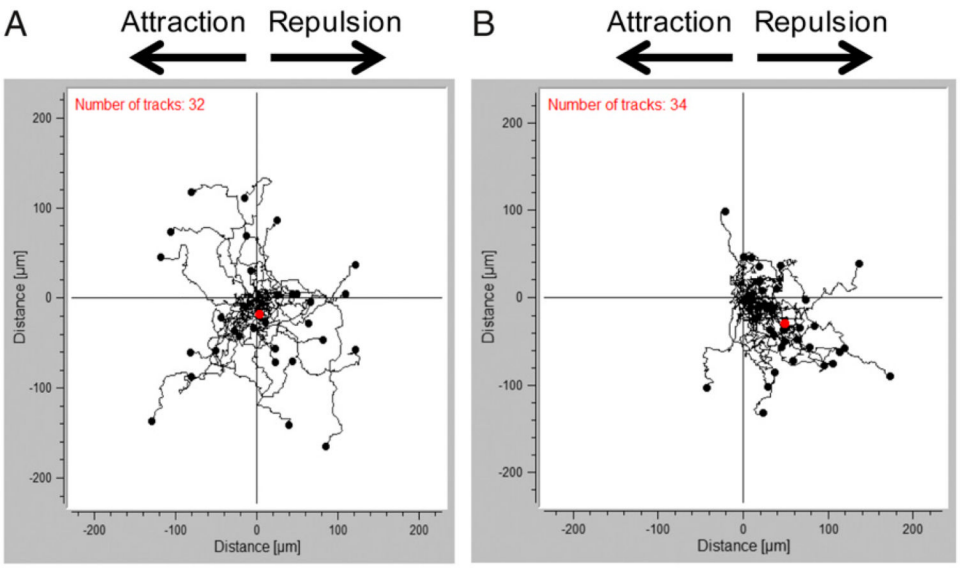

Figure 2.

Human neutrophils show biased movement away from rDPPIV. Neutrophil migration was measured in the (**A**) absence or (**B**) presence of a 0–1.2 nM rDPPIV gradient. Neutrophils were filmed and tracked (see Methods and Materials) during 10-min periods. Orientation is such that the source of rDPPIV is on the *left*. Graphs are data from one of three independent experiments (see Supplemental Fig. 1 for the other two experiments). Red dots represent the average center of mass for the ending positions of all cells.

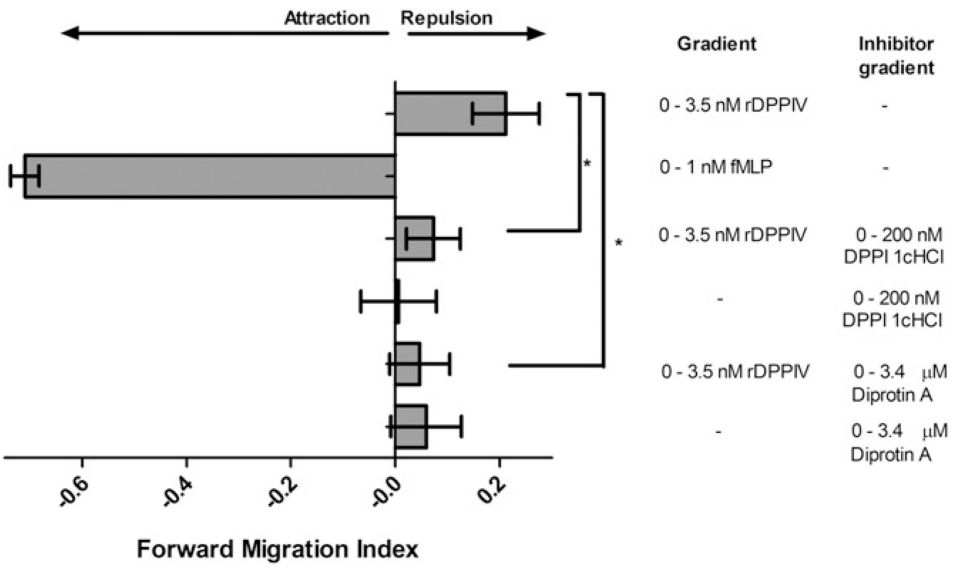

Figure 3.

Inhibitors of DPPIV reduce the chemorepulsion of neutrophils away from DPPIV. The forward migration index is shown for a gradient of DPPIV, fMLP, two DPPIV inhibitors, or DPPIV with the inhibitors. Values are means ± SEM ($n = 3$). *$p < 0.05$ compared with a gradient of DPPIV (by *t* test).

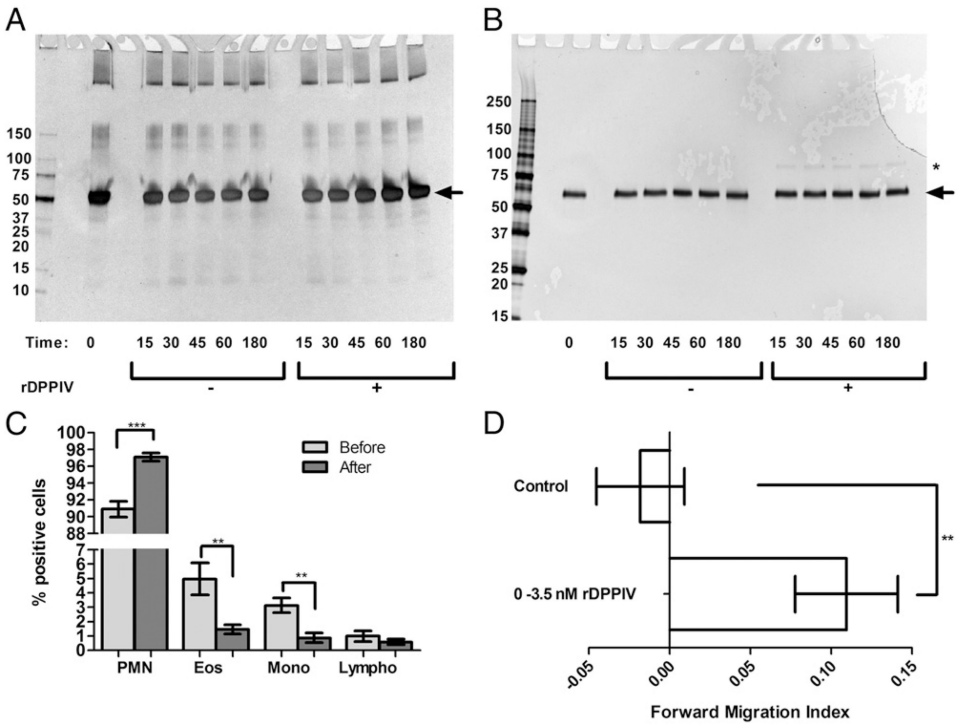

Figure 4.

Purified neutrophils are chemorepulsed by DPPIV. (**A**) BSA-RPMI 1640 (2%) or (**B**) 2% human albumin-RPMI 1640 was incubated with (+) or without (−) 300 ng/ml rDPPIV for 3 h. Time at which samples were taken is given in minutes. Gels were silver stained to identify cleavage products. Molecular masses in kilodaltons are indicated at *left*, * indicates the position of DPPIV, and the arrow indicates the position of albumin. (**C**) Isolated neutrophils were further purified by CD244 depletion. Purity was determined by morphology. Values are means ± SEM ($n = 7$). **$p < 0.01$, ***$p < 0.001$ for percentages after depletion versus percentages before depletion (by *t* test). (**D**) The forward migration index is shown for a DPPIV gradient on purified neutrophils in 2% human albumin-RPMI 1640 buffer. Values are means ± SEM ($n = 7$). **p < 0.01 versus values from the control (two-tailed unpaired *t* test). Eos, eosinophils; Lympho, lymphocytes; Mono, monocytes; PMN, polymorphonuclear neutrophil.

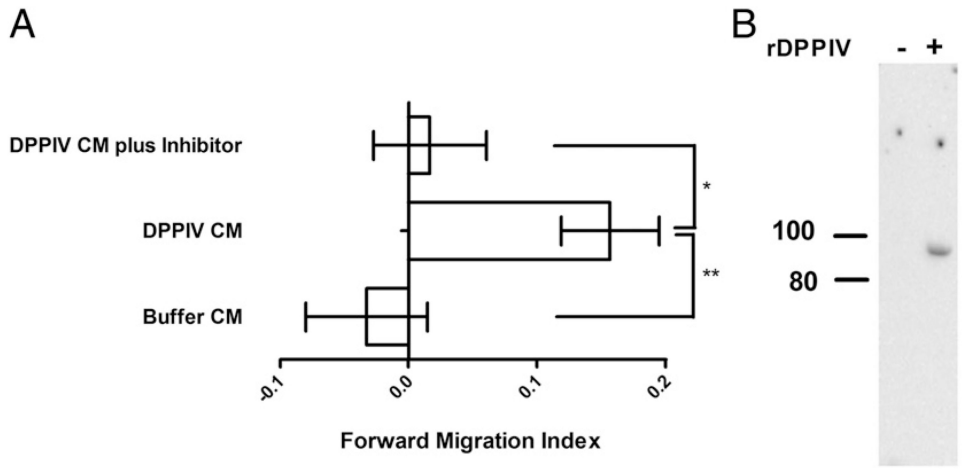

Figure 5.

Effect of neutrophil-conditioned media on chemorepulsion. (**A**) The forward migration index is shown for gradients of conditioned media from DPPIV-treated neutrophils (DPPIV CM), gradients of this material treated with DPPIV inhibitor, and gradients of conditioned media from buffer-treated neutrophils (Buffer CM). Values are means ± SEM ($n = 4$). *$p < 0.05$, **$p < 0.01$ versus values from the control (two-tailed unpaired t test). (**B**) A Western blot of conditioned media using anti-DPPIV Abs. The position of molecular mass standards (in kilodaltons) is indicated on the *left*.

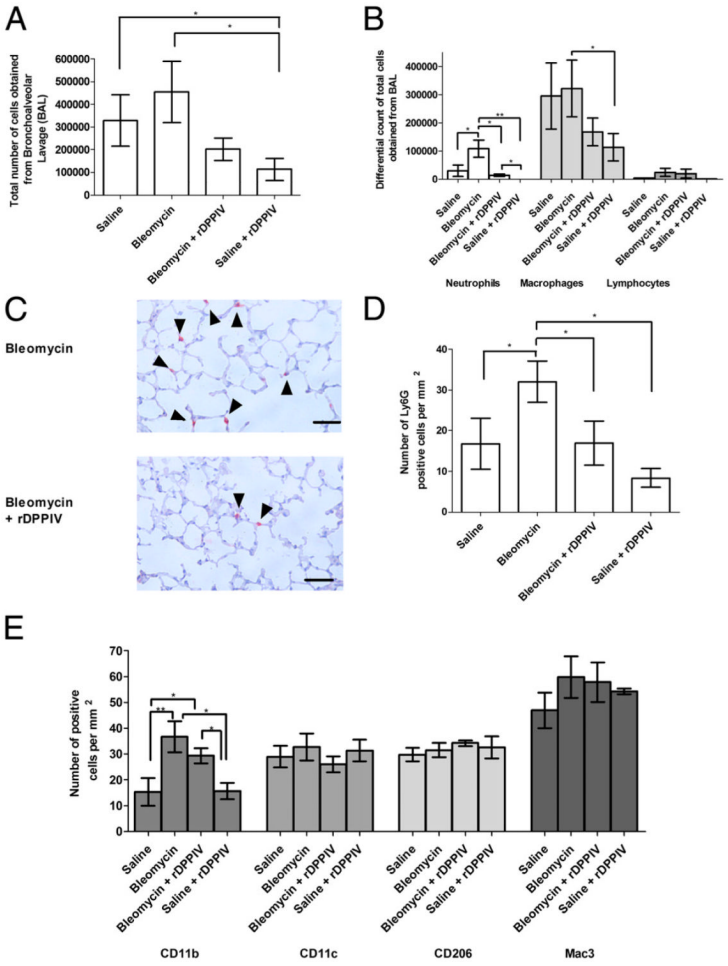

Figure 6.

DPPIV reduces the number of neutrophils in bleomycin-treated lungs. Mice were treated with 3 U/kg bleomycin by oropharyngeal aspirat ion on day 0. On day 1, mice were treated with oropharyngeal aspiration of 0.9 μg human rDPPIV or an equal volume of buffer. Mice were sacrificed on day 3 and cells were collected by BAL. (**A**) The total number of cells collected from the BAL. Values are means ± SEM ($n = 4$ for bleomycin and bleomycin plus DPPIV; $n = 3$ for saline and saline plus DPPIV). *$p < 0.05$ (*t* test) (**B**) The total number of neutrophils, macrophages, and lymphocytes obtained in the BAL for the above experimental groups. Values are means ± SEM ($n = 4$ for bleomycin and bleomycin plus DPPIV; $n = 3$ for saline and saline plus DPPIV). *p < 0.05, **p < 0.01 (by paired one-tailed *t* test). (**C**) Lung sections were stained with anti-mouse Ly6G to detect neutrophils. Arrows indicate $Ly6G^+$ cells. Scale bars, 50 μm. (**D**) Counts of $Ly6G^+$ cells in lung sections. Values are means ± SEM ($n = 4$ for bleomycin and bleomycin plus DPPIV; $n = 3$ for saline and saline plus DPPIV). *$p < 0.05$ (by paired two-tailed *t* test. (**E**) Counts of CD11b, CD11c, CD206, or CD107b (Mac3)-positive cells in lung sections. Values are means ± SEM (n =3). *$p < 0.05$, **$p < 0.01$ (by paired two-tailed *t* test).

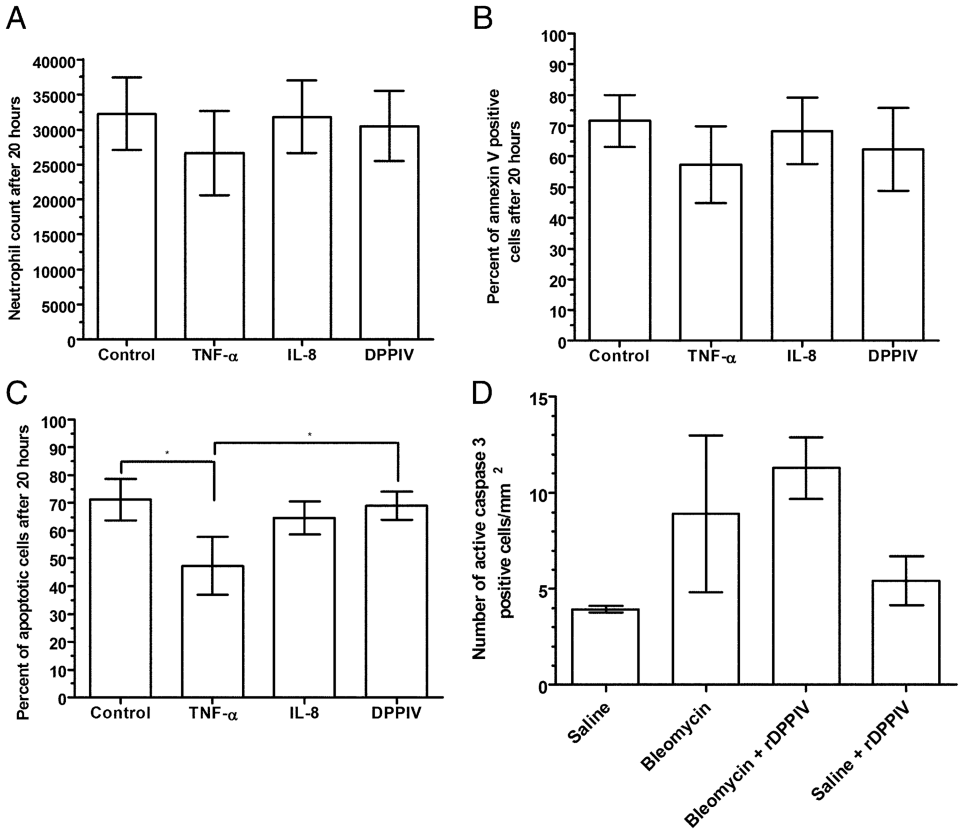

Figure 7.

DPPIV does not regulate neutrophil survival. Human neutrophils were incubated for 20 h in the presence or absence of TNF-α, IL-8, or DPPIV. Values are means ± SEM. (**A**) Neutrophils were identified by their forward and side scatter characteristics and the number of propidium iodide^{-} cells were counted by flow cytometry ($n = 4$). (**B**) The percentage of annexin V^{+} neutrophils was determined by flow cytometry ($n = 3$). (**C**) The percentage of apoptotic neutrophils was assessed by counting nuclei with apoptotic morphology on cytospin preparations ($n = 3$). *$p < 0.05$ (one-way ANOVA). (**D**) Counts of activated caspase-3 in lung sections ($n = 3$).

Table I

The effect of DPPIV on forward migration and directness of neutrophil movement

	Forward Migration Index		Directionality		
rDPPIV Gradient (nM)	Media Control (0 nM rDPPIV)	rDPPIV	Media Control (0 nM rDPPIV)	rDPPIV	No. of Cells Moving toward rDPPIV
0–1.2	0.00 ± 0.03	0.21 ± 0.03***	0.35 ± 0.02	0.39 ± 0.02*	10/93
0–3.5	−0.04 ± 0.04	0.21 ± 0.06***	0.26 ± 0.02	0.50 ± 0.03***	9/55
0–11.7	0.01 ± 0.06	0.15 ± 0.05*	0.47 ± 0.03	0.47 ± 0.02	6/50
4.7–4.7	0.01 ± 0.06	−0.01 ± 0.04	0.47 ± 0.03	0.30 ± 0.02***	N/A
4.7–11.7	−0.02 ± 0.06	0.22 ± 0.06**	0.50 ± 0.03	0.42 ± 0.04*	4/32
9.4–23	−0.01 ± 0.05	0.13 ± 0.05*	0.36 ± 0.03	0.50 ± 0.02***	25/74
0–3.5^{TNF}	−0.02 ± 0.03	0.10 ± 0.03**	0.32 ± 0.02	0.34 ± 0.02	8/81

The data from at least three independent sets of cell population tracks (see Fig. 2 and Supplemental Fig. 1 as examples) were analyzed to determine the forward migration index (FMI) and directionality. FMI is a measure of migration of cells along the gradient, where 0 equals no movement, a positive number equals movement away from the source, and a negative number indicates movement toward the source. Directionality is the ratio of Euclidean distance to accumulated distance. For each gradient, neutrophils from at least three different volunteers were used.

* $p < 0.05$,

** $p < 0.01$,

*** $p < 0.001$ compared with the media control (*t* test).

N/A, not applicable. TNF, gradient of DPPIV with TNF-α–stimulated neutrophils.

Table II
Effect of DPPIV on the average cell speed (μm/min) of neutrophils

rDPPIV gradient (nM)	Media control (0 nM rDPPIV)	rDPPIV
0–1.2	27 ± 1	26 ± 1
0–3.5	23 ± 1	23 ± 1
0–11.7	24 ± 2	25 ± 2
4.7–4.7	17 ± 1	16 ± 1
4.7–11.7	17 ± 1	18 ± 2
9.4–23	17 ± 1	17 ± 1

The data from at least three independent sets of cell population tracks (see Fig. 2 and Supplemental Fig. 1) were used to determine the average speed of neutrophils. Values are means ± SEM ($n = 3$ or more).

Table III

Percentage of cells in the population moving in a biased direction over 10 min

	P_0		P_T		P_A	
rDPPIV Concentration Gradient (nM)	**Control**	**rDPPIV**	**Control**	**rDPPIV**	**Control**	**rDPPIV**
0–1.2	0.39 ± 0.14	0.54 ± 0.02	0.32 ± 0.08	0.16 ± 0.01*	0.29 ± 0.06	0.31 ± 0.02
0–3.5	0.27 ± 0.13	0.28 ± 0.08	0.39 ± 0.08	0.27 ± 0.04	0.34 ± 0.06	0.45 ± 0.06*
0–11.7	0.10 ± 0.03	0.13 ± 0.06	0.46 ± 0.01	0.35 ± 0.02*	0.44 ± 0.03	0.52 ± 0.05
4.7–4.7	0.17 ± 0.07	0.20 ± 0.05	0.44 ± 0.03	0.43 ± 0.03	0.39 ± 0.04	0.37 ± 0.03
4.7–11.7	0.19 ± 0.06	0.22 ± 0.06	0.44 ± 0.03	0.26 ± 0.05*	0.38 ± 0.04	0.53 ± 0.02*
9.4–23	0.29 ± 0.02	0.22 ± 0.06	0.39 ± 0.03	0.38 ± 0.03	0.33 ± 0.02	0.40 ± 0.08
$0–3.5^{TNF}$	0.26 ± 0.04	0.26 ± 0.03	0.38 ± 0.04	0.31 ± 0.03	0.36 ± 0.01	0.43 ± 0.02*

The data from at least three independent sets of cell population tracks (see Fig. 2 and Supplemental Fig. 1 for examples) were used to determine the probability of cell movement toward or away from the source of DPPIV. P_A and P_T are the probabilities that a cell would move away from or toward the source of DPPIV, respectively, in a 13-s interval. P_0 is the probability that a cell will not move. P_A and P_T are statistically significantly different in all DPPIV gradients at $p < 0.05$ (*t* test), except for 0–11.7 nM DPPIV, which is significant at $p < 0.01$. In the controls, P_A and P_T are statistically significant only in the 4.7–11.7 and 9.4–23 nM controls ($p < 0.05$).

TNF, Gradient of DPPIV with TNF-α–stimulated neutrophils.